

# Training-Free Acceleration for Document Parsing Vision-Language Model with Hierarchical Speculative Decoding

Wenhui Liao<sup>1,2†</sup>, Hongliang Li<sup>1,2†</sup>, Pengyu Xie<sup>2,4</sup>, Xinyu Cai<sup>2</sup>, Yufan Shen<sup>2</sup>, Yi Xin<sup>2</sup>,  
 Qi Qin<sup>2</sup>, Shenglong Ye<sup>2</sup>, Tianbin Li<sup>2</sup>, Ming Hu<sup>2</sup>, Junjun He<sup>2</sup>, Yihao Liu<sup>2</sup>,  
 Wenhui Wang<sup>2</sup>, Min Dou<sup>2</sup>, Bin Fu<sup>2,3\*</sup>, Botian Shi<sup>2\*</sup>, Yu Qiao<sup>2\*</sup>, Lianwen Jin<sup>1\*</sup>

<sup>1</sup>South China University of Technology, Guangzhou, China

<sup>2</sup>Shanghai Artificial Intelligence Laboratory, Shanghai, China

<sup>3</sup>Shenzhen Institute of Advanced Technology, CAS, Shenzhen, China

<sup>4</sup>Nanjing University, Nanjing, China

{eelwh, eehongliangli}@mail.scut.edu.cn, eelwjin@scut.edu.cn

{fubin, shibotian, qiaoyu}@pjlab.org.cn

## Abstract

*Document parsing is a fundamental task in multimodal understanding, supporting a wide range of downstream applications such as information extraction and intelligent document analysis. Benefiting from strong semantic modeling and robust generalization, VLM-based end-to-end approaches have emerged as the mainstream paradigm in recent years. However, these models often suffer from substantial inference latency, as they must auto-regressively generate long token sequences when processing long-form documents. In this work, motivated by the extremely long outputs and complex layout structures commonly found in document parsing, we propose a training-free and highly efficient acceleration method. Inspired by speculative decoding, we employ a lightweight document parsing pipeline as a draft model to predict batches of future tokens, while the more accurate VLM verifies these draft predictions in parallel. Moreover, we further exploit the layout-structured nature of documents by partitioning each page into independent regions, enabling parallel decoding of each region using the same draft-verify strategy. The final predictions are then assembled according to the natural reading order. Experimental results demonstrate the effectiveness of our approach: on the general-purpose OmniDocBench, our method provides a  $2.42\times$  lossless acceleration for the dots.ocr model, and achieves up to  $4.89\times$  acceleration on long-document parsing tasks. We will release our code to facilitate reproducibility and future research.*

## 1. Introduction

Document parsing [2, 38, 48] converts document images into structured, marked-up text by organizing textual content, mathematical formulas, tables, and figures according to their natural reading order. As a foundational technology, it supports a wide range of applications, including document indexing and retrieval, workflow automation, data governance, and large-scale corpus construction. To enable these applications at scale, document parsing systems are expected to process massive volumes of documents both accurately and efficiently, which remains a major challenge.

Recent progress in document parsing roughly falls into three categories: pipeline-based [26, 30, 40], end-to-end [2, 31, 42], and hybrid [13, 22, 29] approaches. Pipeline-based methods decompose the parsing workflow into multiple sub-tasks—such as layout analysis, reading-order prediction, text recognition, formula recognition, and table parsing—each addressed by a lightweight specialized model. This modularity enables components such as text, formula, and table recognition to run in parallel across different regions, delivering high computational efficiency. End-to-end approaches, typically built on vision–language models (VLMs) [1, 7, 19, 24], input an image and directly generate the full parsing output. These models feature a clean architecture and benefit from the strong semantic modeling capabilities of VLMs. However, their decoding is inherently slow for long outputs because autoregressive decoding generates tokens sequentially, causing latency to scale approximately linearly with sequence length. Hybrid approaches aim to combine the advantages of both paradigms by first performing layout analysis to segment a page into semantic regions, which are then parsed in parallel by a single

<sup>†</sup>Equal contribution.

<sup>\*</sup>Co-corresponding authors.

VLM. Although this reduces overall latency, each region is still decoded autoregressively, leaving a residual bottleneck. Moreover, the multi-stage structure typically prevents true end-to-end optimization and limits compatibility with recent improvements—such as RL-based parsing enhancements [32, 41]—that assume end-to-end training.

In this paper, we propose a training-free, inference-time acceleration method for end-to-end document parsing, achieving near-lossless speedups without modifying the model architecture or training procedure. To mitigate the latency bottleneck of autoregressive decoding, we draw inspiration from speculative decoding [5, 18, 36, 47], which trades additional FLOPs for a shorter latency-critical path during generation. Specifically, a lightweight draft model predicts a batch of future tokens, and the expensive target model verifies them in parallel. If the target model agrees with the draft within a certain tolerance, decoding skips ahead by multiple tokens; otherwise, it resumes from the point of disagreement. By increasing computational intensity to better utilize GPU resources, verifying multiple tokens in parallel does not substantially degrade per-step efficiency. Combined with the reduction in decoding steps, this yields significant overall acceleration.

Considering the layout-structured nature of documents, to further maximize the speedup in document parsing, we introduce a two-stage local-to-global, hierarchical speculative decoding framework and employ a lightweight pipeline-based method to efficiently generate both draft outputs and layout analysis results. Specifically, the first stage is the region-level local verification stage, where we segment the page into semantic regions via layout analysis from a pipeline model and verify them in parallel with the end-to-end parser. For each region, the pipeline’s predictions serve as speculative drafts. While this parallel, region-wise verification yields high throughput and lower latency, residual within-region errors and cross-region inconsistencies may still remain due to (i) missing global page context, (ii) distribution shift from cropped-region inputs relative to predominantly full-page training, and (iii) inaccuracies in the pipeline’s layout analysis. To address these issues, the second stage (page-level global verification stage) performs a single full-page pass guided by the Stage-1 drafts. Because these drafts are substantially more accurate after the first stage, the second stage only needs a small number of multi-token verification steps to complete decoding. This hierarchical design markedly reduces decoding steps while maintaining near-lossless accuracy.

By leveraging a lightweight pipeline-based method, we prepare page-wide, region-level drafts in one shot, thereby achieving substantially higher draft-preparation throughput than step-by-step refreshing in standard speculative decoding. However, the lightweight pipeline computes fixed drafts *once per page* and they remain unchanged during

verification. In contrast, standard speculative decoding refreshes its drafts at every step to stay synchronized with the target prefix. As a result, our fixed drafts may become unsynchronized, causing mismatches in ordering, granularity, and span boundaries. We address this with windowed alignment and tree-structured verification, which reliably evaluate multiple alternatives in a single parallel multi-token step.

We evaluate our approach on OmniDocBench v1.5 [29], olmOCR-Bench [31], and Ocean-OCR-Bench [6] using multiple end-to-end parsers, including dots.ocr [34], HunyuanOCR [37], Qwen3-VL-8B [39], and Qwen3-VL-2B [39]. Our method delivers significant lossless acceleration, consistently achieving speedups without degrading parsing accuracy across different models, document types, and languages. In particular, on the state-of-the-art end-to-end parser dots.ocr, we obtain speedups of  $2.42\times$ ,  $2.27\times$ , and  $3.68\times$  on OmniDocBench v1.5 [29], olmOCR-Bench [31], and Ocean-OCR-Bench [6], respectively. These gains stem from a plug-and-play framework that requires no architectural changes or retraining, enabling seamless integration with existing end-to-end parsers. To the best of our knowledge, this is the first work to introduce speculative decoding into document parsing, opening up new avenues for efficient document intelligence systems.

In conclusion, our main contributions are three-fold:

- We propose a hierarchical speculative decoding framework tailored to end-to-end document parsing, achieving substantial speedups with a two-stage, local-to-global verification strategy that leverages document layout.
- We introduce high-throughput draft generation via a lightweight pipeline, together with windowed alignment and tree-structured verification to address draft-target misalignment.
- Experiments on multiple end-to-end parsers and benchmarks show that our training-free, plug-and-play approach yields up to  $4.89\times$  speedup with near-lossless accuracy, opening a new avenue for document parsing acceleration.

## 2. Related Works

### 2.1. Document Parsing

**Traditional Pipelines.** Document parsing [27, 30, 40] is inherently heterogeneous: pages mix text, mathematical expressions, tables, charts, and figures arranged in widely varying layouts and reading orders. To address these challenges, early systems decomposed the task into submodules—layout analysis, reading-order estimation, text recognition, formula recognition, table recognition, and final assembly. Representative toolkits such as Marker [30], MinerU [40], PP-StructureV3 [9], and Docling [26] exemplify this design. For example, MinerU [40] begins with

layout detection to partition a page into semantically labeled regions. It then routes each region to task-specific recognizers (text, equations, tables) and reconstructs the reading order to produce a consolidated Markdown result. These pipelines deliver practical throughput and engineering flexibility: lightweight specialists process layout regions in parallel, and modules can be swapped without retraining. However, cross-stage error propagation and limited submodule robustness can lead to failures on complex documents.

**End-to-End Approaches.** Recent work [4, 25] has shifted toward end-to-end document parsing with a single autoregressive vision–language model (VLM). The model ingests a page image and directly emits structured markup, jointly modeling text, tables, equations, and reading order under a unified objective and long-context decoding. Early efforts such as Nougat [2] targeted scientific articles, converting pages into lightweight LaTeX/Markdown-style markup. GOT [42] generalizes this paradigm to broader document types and richer elements (e.g., molecular formulas, sheet music, geometric shapes, and charts) while emphasizing efficiency via a highly compressed vision encoder paired with a 0.5B decoder. Subsequent models such as Ocean-OCR [6], olmOCR [31], dots.ocr [34] and HunyuanOCR [37] push accuracy by adopting native-resolution encoders and training on larger, higher-quality, and more diverse corpora. Beyond supervised learning, researchers have also begun to explore reinforcement learning and verifiable training signals: Infinity-Parser [41] optimizes layout fidelity with rewards on edit distance, paragraph counts, and structural consistency, whereas olmOCR 2 [32] uses binary unit tests as a programmatic reward signal. More recently, DeepSeek-OCR [43] reduces token budgets by compressing visual context into fewer vision tokens before text decoding, shortening sequences and latency. Overall, end-to-end parsers now achieve competitive parsing accuracy, yet autoregressive decoding over long outputs remains a key inference bottleneck.

**Hybrid Approaches.** Hybrid parsers [8, 13, 22, 29] combine the efficiency of pipelines with the semantic capacity of end-to-end models. They first run a lightweight layout stage to segment and order semantic regions on the page, then parse each region with a vision–language model, and finally stitch the results into full-page markup. Representative systems include MonkeyOCR [22], Dolphin [13], MinerU2.5 [29], and PaddleOCR-VL [8]. These designs shorten sequences per decode call and exploit concurrency, but still decode tokens autoregressively within each region. As a result, long text blocks remain slow, and mismatches between the analysis stage and the generator can propagate errors. In addition, the multi-stage design complicates end-to-end optimization and is less compatible with recent training-time improvements that assume joint training (e.g., RL-based parsing [32, 41]).

## 2.2. Speculative Decoding

Speculative decoding [5, 18, 35, 49] accelerates autoregressive generation with a draft–verify scheme: a fast drafter proposes multiple next tokens and the target model verifies them in a single forward pass using rejection sampling, which preserves the target distribution while reducing sequential steps. Methods are best organized along two axes. The first axis is who drafts: external drafters use a separate small model; internal drafters augment the target model with lightweight drafting modules, including Medusa [3], EAGLE [20], and EAGLE-2 [21]; self-speculative methods [12], also called early-exit, let the same network draft with truncated layers and then verify with the full stack. The second axis is what is drafted: linear chunks or a branching tree [28]. In linear drafting, the drafter predicts a single  $k$ -token continuation and the verifier accepts the longest matching prefix before the first mismatch. In tree drafting [28], the drafter explores multiple alternatives at one or more steps, forming a token tree that is verified in parallel; this typically raises per-round acceptance—especially for long outputs—at the cost of extra draft compute and memory. Extensions to VLMs [14, 16, 23, 45] adapt these ideas to visual inputs and report around twofold throughput gains on systems such as LLaVA while maintaining quality. Despite this progress, speculative decoding remains underexplored for document parsing, where long and highly structured outputs make the approach especially promising.

## 3. Methodology

We propose a training-free, inference-time acceleration method for end-to-end document parsers via *hierarchical speculative decoding*. A lightweight document parsing pipeline first produces layout analysis results and region-level text predictions (drafts). The end-to-end parser then verifies these drafts in a two-stage manner: (1) The region-level local verification stage verifies drafts on the cropped region in parallel and aggregates the outputs into a list of page-level draft; (2) The page-level global verification stage performs page-level verification in a small number of multi-token steps. In the following, we first introduce this two-stage hierarchical framework in Section 3.1, and then provide details of our verification operator in Section 3.2.

### 3.1. Hierarchical Speculative Decoding Framework

Given the page image  $x$ , the end-to-end parser  $p_\theta$  autoregressively produces tokens  $y_t$  forming a sequence  $\mathbf{y} = (y_{1:T})$  that spans text, formulas, tables, and figure markers, with conditional probabilities  $p_\theta(y_t|x, y_{<t})$ . A lightweight pipeline  $q_\phi$  runs once per page and outputs a page layout  $\mathcal{R} = \{r_i\}_{i=1}^M$  with a small set of fixed drafts  $\tilde{\mathcal{Y}}^{(i)} = \{\tilde{\mathbf{y}}^{(i,k)}\}_{k=1}^{K_i}$  for each region  $r_i$ . We denote the verification

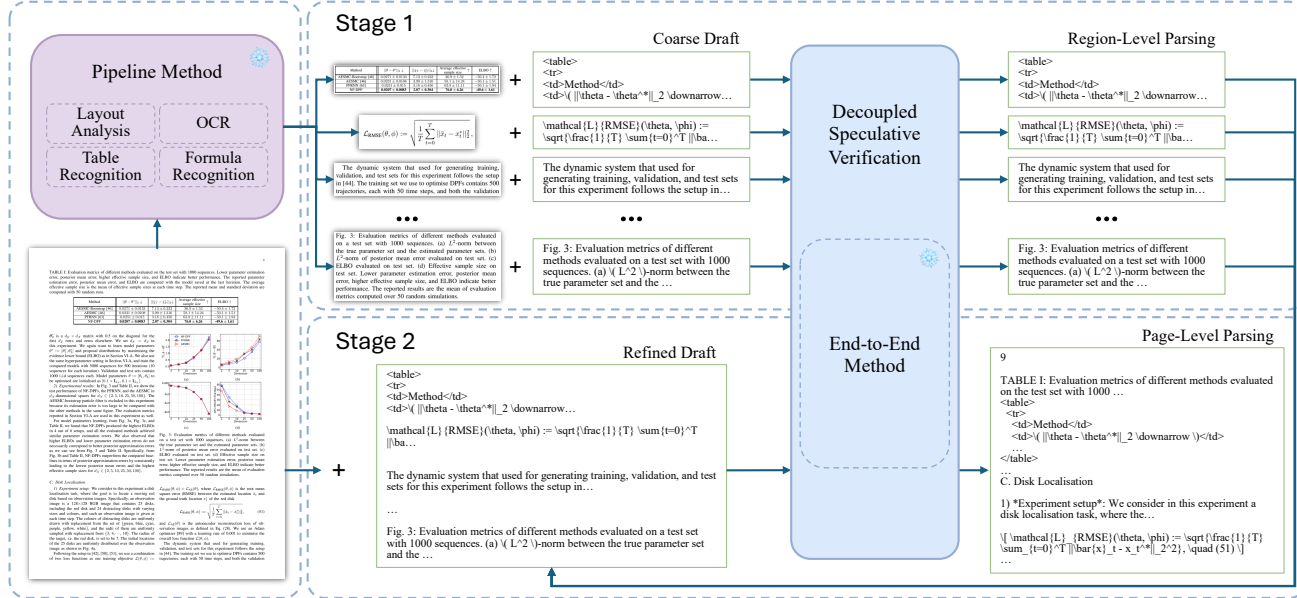


Figure 1. Overview of the proposed hierarchical speculative decoding framework for end-to-end document parsing. A lightweight pipeline first performs layout analysis and emits fixed region drafts. Stage 1 parses region crops in parallel via *Decoupled Speculative Verification* (DSV) to obtain verified outputs; Stage 2 aggregates them into a page-level draft and performs one full-page pass with DSV to finalize the parse. DSV combines windowed alignment and tree-structured verification to evaluate multiple draft alternatives in a single parallel multi-token step.

operator by `SpecDecode`:

$$\hat{y} = \text{SpecDecode}(p_\theta, z, \tilde{y}), \quad (1)$$

which takes the current visual input  $z$  (either a region crop or the full page) with a draft set  $\tilde{y}$ , and returns a verified sequence  $\hat{y}$ . Intuitively, `SpecDecode` treats drafts as proposals and uses the document parser  $p_\theta$  to accept or correct them in multi-token steps (details in Section 3.2). Building on this operator, we instantiate a two-stage hierarchy in which the first stage verifies region drafts in parallel, and the second stage performs a single page-level pass to reconcile context.

**Stage 1 (Region-level Local Verification).** For each  $r_i \in \mathcal{R}$ , let  $z_i = x|_{r_i}$  be the region crop. We verify the corresponding region drafts in parallel:

$$\hat{y}^{(i)} = \text{SpecDecode}(p_\theta, z_i, \tilde{y}^{(i)}). \quad (2)$$

Parallel region-wise verification provides high throughput and shortens decoding; however, residual errors—both within-region and cross-region—may persist due to (i) the absence of full-page context, (ii) distribution shift induced by cropped-region inputs underrepresented during training, and (iii) inaccuracies in the pipeline’s layout analysis.

**Stage 2 (Page-level Global Verification).** To address these residual errors, we aggregate Stage 1 outputs into a

page-level draft set and perform a single pass on the full page:

$$\begin{aligned} \hat{y}^{\text{pg}} &= \{\hat{y}^{(i)}\}_i, \\ \hat{y} &= \text{SpecDecode}(p_\theta, x, \hat{y}^{\text{pg}}). \end{aligned} \quad (3)$$

We treat  $\hat{y}^{\text{pg}}$  as an *unordered* collection; the final reading order is resolved by  $p_\theta$  during verification. In other words, Stage 1 outputs act as high-quality page-level drafts that allow Stage 2 to complete in only a few multi-token steps.

### 3.2. Decoupled Speculative Verification

Classical speculative decoding refreshes the draft synchronously at every step so that the draft continuation exactly follows the current target prefix. In contrast, our setting is *decoupled*: the lightweight pipeline computes fixed drafts *once per page* and they remain unchanged during verification. This decoupling introduces misalignment in order, granularity, and span boundaries. We therefore design a two-part mechanism: (i) align fixed drafts to the evolving target prefix via a short *reference window*, and (ii) verify *multiple* aligned candidates in one forward pass using a *prefix-tree* formulation with a specialized attention mask. See Fig. 2 for a visualization of decoupled speculative verification.

**Preliminaries.** For any sequence  $a$ , slice notation  $a_{p:q}$  denotes the contiguous subsequence  $(a_p, \dots, a_q)$ , and  $|a|$  de-

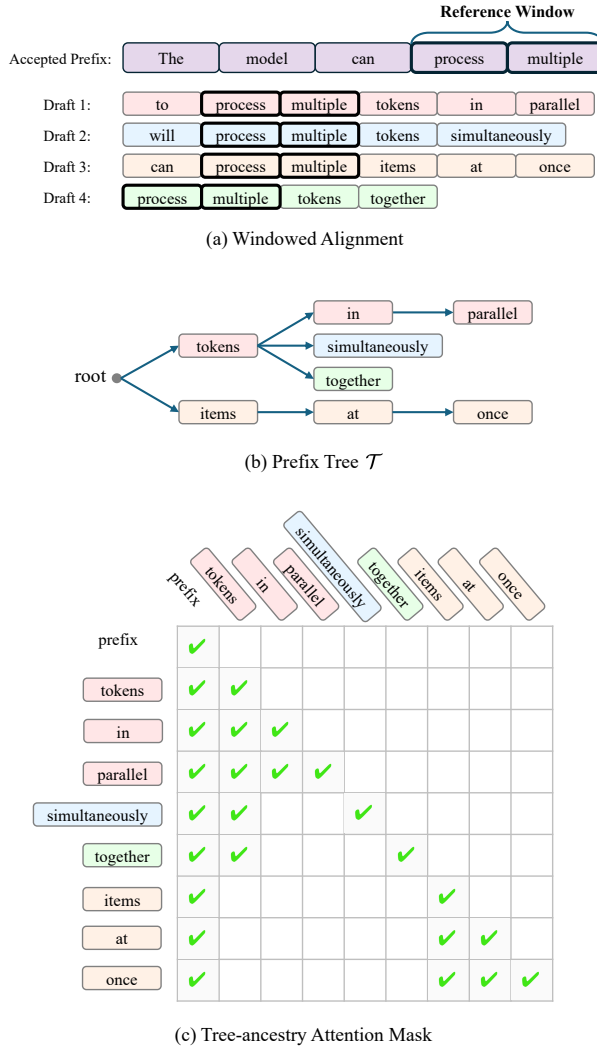


Figure 2. Visualization of decoupled speculative verification. (a) Windowed alignment matches a reference window (bold) from the accepted prefix against multiple drafts to extract candidate continuations. (b) Prefix tree organizes candidates by merging common prefixes. (c) Tree-ancestry attention mask enables parallel verification, where tokens attend only to the prefix and their ancestors (green checkmarks indicate allowed attention).

notes its length (in tokens).

**Windowed alignment.** At decoding step  $t$ , let  $\hat{\mathbf{y}}_{1:t}$  denote the accepted prefix. Let  $n$  denote the desired window length. As shown in Fig. 2(a), we take the reference window to be the most recent  $n$  tokens of the accepted prefix. Thus, the reference window can be expressed as  $\mathbf{w} = \hat{\mathbf{y}}_{t-n+1:t}$ .

We slide the token sequence of the reference window  $\mathbf{w}$  across the draft  $\tilde{\mathbf{y}}$  and record every start position where it matches, forming  $\mathcal{J}(\tilde{\mathbf{y}})$ :

$$\mathcal{J}(\tilde{\mathbf{y}}) = \{ j \mid \tilde{\mathbf{y}}_{j:j+n-1} = \mathbf{w} \text{ and } 1 \leq j \leq L - n + 1 \}, \quad (4)$$

where  $j$  indexes the start position of each match and  $L$  is the length of the draft  $\tilde{\mathbf{y}}$ . We then extract the suffixes strictly following each matched window and collect them across all drafts in  $\tilde{\mathcal{Y}}$ :

$$\mathcal{C} = \left\{ \tilde{\mathbf{y}}_{j+n:L} \mid \tilde{\mathbf{y}} \in \tilde{\mathcal{Y}} \text{ and } j \in \mathcal{J}(\tilde{\mathbf{y}}) \text{ and } j + n \leq L \right\}. \quad (5)$$

where  $\tilde{\mathbf{y}}_{j+n:L}$  denotes the continuation strictly after the matched window, and  $\tilde{\mathcal{Y}}$  is the set of drafts.

**Prefix-tree batching.** When the number of candidates  $|\mathcal{C}| > 1$ , verifying each candidate independently is redundant. To address this issue, we organize  $\mathcal{C}$  into a prefix tree  $\mathcal{T}$  that merges common prefixes, thereby enabling parallel verification. As shown in Fig. 2(b), each node  $v$  in  $\mathcal{T}$  represents a unique prefix. Let  $\pi(v)$  denote the token sequence along the path from the root to  $v$ . For example, if the node  $v$  is *parallel* (in Fig. 2(b)), then we have  $\pi(v) = \text{tokens in parallel}$ .

For any node  $v$ , we define the set of possible next tokens  $\text{Next}(v)$  as

$$\text{Next}(v) = \left\{ \mathbf{c}_{|\pi(v)|+1} \mid \mathbf{c} \in \mathcal{C} \text{ and } \mathbf{c}_{1:|\pi(v)|} = \pi(v) \right\}. \quad (6)$$

Among all sequences  $\mathbf{c} \in \mathcal{C}$  that share the prefix  $\pi(v)$ ,  $\text{Next}(v)$  collects the distinct tokens that appear immediately after this prefix. In Fig. 2(b), for the node corresponding to the prefix *tokens*, we have  $\text{Next}(v) = \{\text{in}, \text{simultaneously}, \text{together}\}$ . For each token  $u \in \text{Next}(v)$ , there exists a unique node  $w$  with  $\pi(w) = \pi(v) \oplus u$ , where  $\oplus$  denotes concatenation. We record  $w$  as  $\text{child}(v, u)$ , and then create a directed edge from  $v$  to  $\text{child}(v, u)$ .

With the above definition, we construct the prefix tree as follows: The construction begins at the root, which represents the empty prefix ( $\pi(\text{root}) = \emptyset$ ), and is applied recursively to each newly created child. The process continues until every sequence in  $\mathcal{C}$  is represented by a path from the root to a leaf. The resulting prefix tree compactly encodes all candidate continuations by sharing common prefixes.

To enable parallel verification, we linearize  $\mathcal{T}$  into a packed sequence and apply a *tree-ancestry attention mask*: a token at node  $v$  may only attend to the accepted prefix  $\hat{\mathbf{y}}_{1:t}$  and tokens on the ancestor path of  $v$ , as shown in Fig. 2(c).

This enables processing all candidate paths in one forward pass while preserving autoregressive conditioning.

**Verification and acceptance.** Let  $\tau \in (0, 1)$  be the acceptance threshold. For any node  $v$ , the model produces next-token distributions

$$p_\theta(\cdot \mid z, \hat{\mathbf{y}}_{1:t} \oplus \pi(v)), \quad (7)$$

where  $z$  is the current visual input, either a region crop or the full page. We perform a greedy traversal on the prefix tree to find the final accepted token sequence.

At each step, we select the most probable next token among the candidate set  $\text{Next}(s)$ :

$$u^* = \arg \max_{u \in \text{Next}(s)} p_\theta(u \mid z, \hat{\mathbf{y}}_{1:t} \oplus \pi(s)), \quad (8)$$

where  $s$  is the current node. Let  $\mathcal{V}$  denote the vocabulary. We define  $\hat{u} \in \mathcal{V}$  to be the token with the highest model probability under the current context:

$$\hat{u} = \arg \max_{u \in \mathcal{V}} p_\theta(u \mid z, \hat{\mathbf{y}}_{1:t} \oplus \pi(s)). \quad (9)$$

We accept  $u^*$  and move to its child node if

$$\frac{\log p_\theta(\hat{u} \mid z, \hat{\mathbf{y}}_{1:t} \oplus \pi(s))}{\log p_\theta(u^* \mid z, \hat{\mathbf{y}}_{1:t} \oplus \pi(s))} \geq \tau. \quad (10)$$

If the condition fails, we stop at the current node  $s$ . Additionally, if  $s$  is a leaf node, there is no admissible next token and the traversal stops at  $s$ . Upon termination, we update the accepted prefix:

$$\hat{\mathbf{y}}_{1:t_{\text{new}}} = \hat{\mathbf{y}}_{1:t} \oplus \pi(s) \oplus \hat{u}. \quad (11)$$

By organizing candidates into a tree and verifying them in parallel, each step can accept multiple tokens at once, substantially reducing the number of decoding steps. Tree-structured batching increases per-step compute utilization without elongating the latency-critical path, yielding significant wall-clock speedup. The decoupled design leverages the high-throughput pipeline while keeping the target model as the arbiter that corrects draft errors.

## 4. Experiments

### 4.1. Datasets

We evaluate on three public benchmarks: OmniDocBench v1.5 [29], olmOCR-Bench [31], and Ocean-OCR-Bench [6]. OmniDocBench v1.5 [29] contains 1,355 PDF pages spanning nine document types and provides rich supervision for document parsing, including 15 block-level categories and 4 span-level elements with text, LaTeX formulas, tables, reading-order annotations, and page/block attributes. We follow the official end-to-end evaluation setup. olmOCR-Bench [31] includes 1,403 PDFs paired with 7,010 unit tests that check properties of PDF-to-Markdown conversion such as content presence, natural reading order, table fidelity, and mathematical expressions. We report the official aggregate score under its evaluation protocol. Ocean-OCR-Bench [6] is a bilingual page-level evaluation built from 200 document images (100 English and 100 Chinese). The official metrics include normalized edit distance, F1, precision, recall, BLEU, and METEOR; we adopt the same protocol.

### 4.2. Metrics

For a comprehensive evaluation, we report three efficiency-related metrics: Decoding Speedup, End-to-End Speedup, and Average Acceptance Length.

**Decoding Speedup.** Decoding Speedup measures acceleration of the latency-critical generation loop:

$$\text{SR}_{\text{decode}} = \frac{T_{\text{decode}}^{\text{AR}}}{T_{\text{decode}}^{\text{Spec}}}. \quad (12)$$

Here  $T_{\text{decode}}^{\text{AR}}$  and  $T_{\text{decode}}^{\text{Spec}}$  are wall-clock times for standard autoregressive decoding and our speculative decoder, respectively, under identical hardware, precision, batch size, and caching. Unless otherwise noted,  $T_{\text{decode}}$  *includes* the draft model’s forward passes used for speculation, target-model parallel verification, accept/reject control flow (including rollbacks) and KV-cache maintenance, as well as any communication overheads; it *excludes* disk I/O, non-generative preprocessing, and prefill that is not executed inside the decoding loop.

**End-to-end Speedup.** To reflect user-perceived latency in multimodal settings, we also report end-to-end Speedup:

$$\text{SR}_{\text{e2e}} = \frac{T_{\text{full}}^{\text{AR}}}{T_{\text{full}}^{\text{Spec}}}, \quad (13)$$

where  $T_{\text{full}}$  measures time from page image input to final markup, thereby *including* vision/prefill computation (e.g., visual encoder and text prefill), while still excluding disk I/O. Draft generation triggered specifically to enable speculation (e.g., per-region drafts) is counted in both  $\text{SR}_{\text{decode}}$  and  $\text{SR}_{\text{e2e}}$ .

**Average Acceptance Length.** To quantify how many decoding steps are saved by speculation, we report the Average Acceptance Length (AAL). For verification step  $i$ , let  $a_i$  denote the number of consecutive draft tokens accepted by the target model before the first mismatch (full rejection gives  $a_i = 0$ ). Then

$$\text{AAL} = \frac{1}{N} \sum_{i=1}^N a_i, \quad (14)$$

with  $N$  the number of verification steps. Larger AAL indicates more tokens skipped per step and thus higher potential speedup, though realized SR also depends on per-step verification overhead and parallel efficiency.

### 4.3. Implementation Details

We validate the proposed acceleration method on several mainstream end-to-end parsers, including dots.ocr [34], HunyuanOCR [37], Qwen3-VL-2B [39], and Qwen3-VL-8B [39]. All experiments are conducted on NVIDIA A100 GPUs. For a fair comparison, all methods are evaluated under the same Hugging Face Transformers stack [44], with

Table 1. Acceleration across different models on OmniDocBench v1.5. Results are reported for our proposed Hierarchical Speculative Decoding. AAL denotes the average number of accepted draft tokens per verification step;  $SR_{decode}$  is the decode-only speedup (draft generation + verification);  $SR_{e2e}$  is the end-to-end page-level latency speedup (including vision/prefill stages). \* indicates that samples with output length  $>2048$  tokens are excluded from the reported metrics to prevent bias in acceleration estimates; see the Supplementary Materials for details.

Model	Parameters	Overall			Slides	Academic Papers	Book	Textbook	Exam Papers	Magazine	Newspaper	Notes	Financial Report
		AAL	$SR_{decode}$	$SR_{e2e}$									
Qwen3-VL-8B	9B	2.48 $\times$	1.42 $\times$	1.38 $\times$	0.89 $\times$	1.54 $\times$	1.02 $\times$	1.13 $\times$	1.40 $\times$	2.45 $\times$	2.17 $\times$	0.82 $\times$	1.69 $\times$
Qwen3-VL-8B*	9B	5.64 $\times$	2.88 $\times$	2.74 $\times$	2.01 $\times$	3.89 $\times$	2.74 $\times$	2.38 $\times$	2.67 $\times$	2.98 $\times$	3.87 $\times$	2.10 $\times$	4.66 $\times$
Qwen3-VL-2B	2B	1.96 $\times$	1.22 $\times$	1.18 $\times$	0.85 $\times$	1.25 $\times$	1.16 $\times$	0.74 $\times$	1.30 $\times$	1.33 $\times$	1.27 $\times$	1.13 $\times$	1.52 $\times$
Qwen3-VL-2B*	2B	4.64 $\times$	2.52 $\times$	2.49 $\times$	1.61 $\times$	2.85 $\times$	2.4 $\times$	2.33 $\times$	2.45 $\times$	2.49 $\times$	3.82 $\times$	1.84 $\times$	1.71 $\times$
HunyuanOCR	0.9B	5.55 $\times$	2.82 $\times$	2.78 $\times$	1.58 $\times$	3.41 $\times$	4.00 $\times$	1.92 $\times$	1.72 $\times$	2.60 $\times$	4.30 $\times$	1.98 $\times$	7.04 $\times$
dots.ocr	3B	4.98 $\times$	2.44 $\times$	2.42 $\times$	1.52 $\times$	3.47 $\times$	2.28 $\times$	2.29 $\times$	2.04 $\times$	2.34 $\times$	2.98 $\times$	1.39 $\times$	4.89 $\times$

Table 2. Acceleration across different models on olmOCR-Bench. Results are reported for our proposed Hierarchical Speculative Decoding. \* indicates that samples with output length  $>2048$  tokens are excluded from the reported metrics to prevent bias in acceleration estimates; see the Supplementary Materials for details.

Model	Parameters	Overall			arXiv Math	Old Scans Math	Tables	Old Scans	Headers Footers	Multi Column	Long Tiny Text
		AAL	$SR_{decode}$	$SR_{e2e}$							
Qwen3-VL-8B	9B	3.89 $\times$	2.04 $\times$	2.01 $\times$	2.31 $\times$	1.20 $\times$	1.54 $\times$	0.69 $\times$	2.61 $\times$	3.58 $\times$	1.37 $\times$
Qwen3-VL-8B*	9B	5.39 $\times$	2.49 $\times$	2.46 $\times$	2.56 $\times$	1.67 $\times$	1.85 $\times$	0.76 $\times$	3.00 $\times$	3.86 $\times$	2.58 $\times$
Qwen3-VL-2B	2B	2.32 $\times$	1.34 $\times$	1.27 $\times$	1.41 $\times$	0.89 $\times$	1.12 $\times$	0.54 $\times$	1.64 $\times$	1.73 $\times$	1.21 $\times$
Qwen3-VL-2B*	2B	6.15 $\times$	2.73 $\times$	2.66 $\times$	2.77 $\times$	1.61 $\times$	2.08 $\times$	0.94 $\times$	3.19 $\times$	4.23 $\times$	2.23 $\times$
dots.ocr	3B	4.03 $\times$	2.30 $\times$	2.27 $\times$	2.11 $\times$	2.10 $\times$	2.45 $\times$	1.58 $\times$	2.70 $\times$	2.11 $\times$	2.61 $\times$

Table 3. Acceleration performance across different models on Ocean-OCR-Bench. Results are reported for our proposed Hierarchical Speculative Decoding.

Model	Parameters	Overall			English	Chinese
		AAL	$SR_{decode}$	$SR_{e2e}$		
Qwen3-VL-8B	9B	7.88 $\times$	6.14 $\times$	6.09 $\times$	5.97 $\times$	8.25 $\times$
Qwen3-VL-2B	2B	4.11 $\times$	3.02 $\times$	2.99 $\times$	2.07 $\times$	4.81 $\times$
dots.ocr	3B	6.79 $\times$	3.79 $\times$	3.68 $\times$	3.61 $\times$	3.75 $\times$

FlexAttention [33] enabled for attention computation. Our pipeline-based method uses PP-StructureV3 [9] by default for layout analysis and to generate region drafts. In Decoupled Speculative Verification, we set the reference-window length to  $n = 3$  and the acceptance threshold to  $\tau = 0.75$ .

#### 4.4. Acceleration Performance Across Diverse Document Types and Models

To comprehensively evaluate the effectiveness of our hierarchical speculative decoding framework, we conduct experiments across three benchmarks (OmniDocBench v1.5, olmOCR-Bench, and Ocean-OCR-Bench) and multiple models, including the specialized document parser dots.ocr and general-purpose VLMs (Qwen3-VL-8B and Qwen3-VL-2B). Tabs. 1 to 3 demonstrate that our method achieves consistent and substantial speedups across diverse settings. On the state-of-the-art end-to-end parser dots.ocr, we achieve end-to-end speedups of  $2.42\times$ ,  $2.27\times$ , and  $3.68\times$

on the three benchmarks respectively, validating the general applicability of our approach. In the following, we focus our analysis on the state-of-the-art end-to-end parser dots.ocr.

**Impact of draft quality.** The acceleration performance varies significantly across document types, ranging from  $1.39\times$  to  $4.89\times$  end-to-end speedup on dots.ocr. This variation primarily stems from differences in the quality of drafts generated by the pipeline. In challenging scenarios with irregular layouts or degraded text, the pipeline generates lower-quality drafts that require more correction steps during verification. For instance, the Notes category in OmniDocBench v1.5, which contains highly variable handwriting styles, yields only  $1.39\times$  speedup. Similarly, Old Scans in olmOCR-Bench, characterized by degraded historical documents, shows limited acceleration at  $1.58\times$ .

Conversely, documents with regular structure allow the pipeline to produce higher-quality drafts, yielding substantial acceleration. The Financial Report category achieves the highest observed end-to-end speedup of  $4.89\times$ , benefiting from regular table layouts, which the pipeline parses accurately. Ocean-OCR-Bench, with its relatively standardized layouts, likewise achieves a  $3.68\times$  speedup.

To further examine how draft quality affects our method, we build on the experiments with HunyuanOCR and evaluate speedups under drafts of varying quality. First, we use drafts produced by the MinerU2-pipeline [40], which

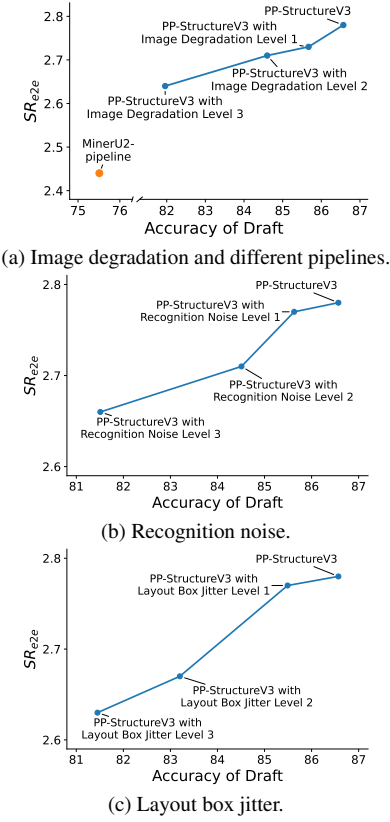


Figure 3. Impact on speedup of draft quality under different perturbations. Draft quality is measured by the draft’s score on OmniDocBench v1.5.

are slightly lower-quality than those from PP-StructureV3. In addition, to more comprehensively study how different pipeline failure modes influence acceleration, we generate drafts of different quality by (1) applying different levels of degradation to the input images of PP-StructureV3, and (2) injecting recognition errors and layout bounding-box jitter into the original PP-StructureV3 outputs to simulate diverse low-quality drafts that may arise in practice. Draft quality is measured by draft’s score on OmniDocBench v1.5. As shown in Fig. 3, as draft quality decreases, the speedup achieved by our method degrades only mildly and consistently remains above  $2.4\times$ . These results demonstrate the robustness and practical applicability of our method under imperfect pipeline-generated drafts across diverse degradation cases.

**Effect of document length.** Document length also influences acceleration performance. Shorter documents like Slides ( $1.52\times$  speedup) offer limited opportunities for multi-token verification, as the fixed front-end cost—image encoding and text prefill—becomes more prominent relative to the total decoding time. In contrast, longer documents such as Newspapers ( $2.98\times$  speedup) better amortize

Table 4. Acceleration achieved by different speculative decoding methods on OmniDocBench v1.5.

Method	OmniDocBench v1.5	
	AAL	SR <sub>e2e</sub>
VSD		5.17 $\times$ 1.06 $\times$
ViSpec	official	1.12 $\times$ 1.09 $\times$
	fine-tuned	1.76 $\times$ 1.29 $\times$
Ours	dots.ocr(based)	4.98 $\times$ 2.42 $\times$
	HunyuanOCR(based)	5.55 $\times$ 2.78 $\times$

Table 5. Average draft generation latency of vanilla speculative decoding (VSD) and our hierarchical speculative decoding on OmniDocBench v1.5.

Method	Average Draft Generation Latency	AAL
VSD	13.07s	5.17 $\times$
Ours	1.99s	4.98 $\times$

these fixed costs across more decoding steps, enabling more efficient acceleration.

**Language independence.** Notably, our method demonstrates consistent performance across languages. As shown in Tab. 3, the speedups for English ( $3.61\times$ ) and Chinese ( $3.75\times$ ) documents are comparable, indicating that our windowed alignment and tree-structured verification mechanisms effectively handle different linguistic characteristics without language-specific tuning.

#### Compared with other speculative decoding methods.

To further demonstrate the effectiveness of our approach, we compare it with representative speculative decoding baselines on OmniDocBench v1.5. Specifically, we implement vanilla speculative decoding [5, 15] using Qwen3-VL-8B as the target model and Qwen3-VL-2B as the drafter. We also compare against the state-of-the-art speculative decoding baseline in vision-aware settings—ViSpec [16], evaluating (i) its official ViSpec-Qwen3-VL-2B drafter, and (ii) a domain-adapted variant where the drafter is further fine-tuned on document parsing data.

As shown in Tab. 4, our method consistently outperforms both vanilla speculative decoding and the SOTA baseline. While our approach achieves an AAL comparable to vanilla speculative decoding (VSD), generating drafts via a pipeline document parser is substantially lower draft-generation latency as reported at Tab. 5, leading to higher end-to-end speedups. Moreover, ViSpec indeed delivers larger speedups than vanilla speculative decoding, and domain-adaptive fine-tuning further improves its performance; however, our method remains significantly faster, highlighting the advantage of our design.

**Combining with the visual token compression method.** Orthogonal to our approach, another line of acceleration methods in document parsing reduces the number of visual tokens via visual token compression (VTC),

Table 6. Acceleration across benchmarks when combining our hierarchical speculative decoding (HSD) with the visual token compression (VTC) method.

Method	OmniDocBench v1.5			olmOCR-Bench			Ocean-OCR-Bench		
	AAL	$SR_{decode}$	$SR_{e2e}$	AAL	$SR_{decode}$	$SR_{e2e}$	AAL	$SR_{decode}$	$SR_{e2e}$
VTC (DeepSeek-OCR)	1.00 $\times$	1.00 $\times$	1.00 $\times$	1.00 $\times$	1.00 $\times$	1.00 $\times$	1.00 $\times$	1.00 $\times$	1.00 $\times$
+ HSD (Ours)	4.72 $\times$	1.51 $\times$	1.56 $\times$	4.65 $\times$	1.39 $\times$	1.41 $\times$	6.36 $\times$	1.87 $\times$	1.91 $\times$

Table 7. Accuracy comparison of the draft model, baseline end-to-end parsers, and our hierarchically accelerated variants across three benchmarks.

Method	OmniDocBench v1.5	olmOCR-Bench	Ocean-OCR-Bench
Pipeline (Draft)	86.73	65.80	85.20
Baseline	88.41	79.90	91.45
dots.ocr	Stage-1 only	70.47	67.30
Stage-1+2 (Ours)	88.81	79.40	92.56

Table 8. Ablation of components of our hierarchical speculative decoding, evaluated with dots.ocr on OmniDocBench v1.5.

Method	AAL	$SR_{decode}$	$SR_{e2e}$
Baseline	1.00 $\times$	1.00 $\times$	1.00 $\times$
+ Page-level Spec. Decoding only	3.49 $\times$	2.11 $\times$	2.09 $\times$
+ Hierarchical Spec. Decoding ( $\tau=1.0$ )	3.87 $\times$	2.37 $\times$	2.34 $\times$
+ Hierarchical Spec. Decoding ( $\tau=0.75$ )	4.98 $\times$	2.44 $\times$	2.42 $\times$

thereby reducing the attention cost and improving inference efficiency; a representative example is DeepSeek-OCR [43]. This naturally raises the question of whether our method can be combined with such token-compression approaches. To investigate this, we integrate our HSD with DeepSeek-OCR. As shown in Tab. 6, HSD provides additional speedups on top of DeepSeek-OCR, demonstrating the plug-and-play nature of our method and its potential to be combined with other acceleration techniques.

Results in Tab. 6 validate that our hierarchical speculative decoding framework provides robust acceleration across diverse benchmarks, highlighting the flexibility and plug-and-play nature of our framework.

#### 4.5. Ablation Study

**Accuracy Analysis of Hierarchical Design.** Tab. 7 validates the effectiveness of our hierarchical design and demonstrates near-lossless acceleration. When using only Stage-1 (region-level verification), performance degrades significantly—dots.ocr drops from 88.41 to 70.47 on OmniDocBench v1.5—due to missing global context and distribution shift from cropped inputs. Stage-2 (page-level verification) is therefore essential, recovering and even slightly improving accuracy (88.81 on OmniDocBench v1.5, 92.56 on Ocean-OCR-Bench). Despite employing tolerance-based draft verification, the final accuracy remains comparable to or better than baseline across all benchmarks, with

minor variations falling within normal variance. These results demonstrate that our hierarchical speculative decoding achieves substantial speedups while maintaining parsing quality.

**Impact of Framework Components.** Tab. 8 presents an ablation study analyzing the contribution of each component on OmniDocBench v1.5. Comparing page-level-only speculative decoding with our hierarchical approach reveals the advantage of the two-stage design: while page-level-only achieves 2.09 $\times$  speedup, our hierarchical method reaches 2.34 $\times$  by exploiting regional parallelism in Stage-1.

The tolerance mechanism ( $\tau = 0.75$ ) shows a measurable effect on draft utilization: exact matching ( $\tau = 1.0$ ) yields an AAL of 3.87 $\times$  due to rejecting minor formatting variations, whereas tolerance-based matching increases AAL to 4.98 $\times$  and raises end-to-end speedup from 2.34 $\times$  to 2.42 $\times$ . This performance gain comes without degrading accuracy, as minor token variations (spacing, punctuation) often represent equivalent semantic content in document parsing. The progression from baseline to our complete framework demonstrates that hierarchical design and tolerance-based verification work synergistically to achieve optimal acceleration.

## 5. Conclusion

In this work, we addressed the fundamental efficiency challenges of VLM-based end-to-end document parsing, which often suffers from substantial inference latency due to extremely long output sequences and complex layout structures. We introduced a training-free and highly efficient acceleration framework inspired by speculative decoding. By leveraging a lightweight document parsing pipeline as a draft model, our method predicts batches of future tokens that are verified in parallel by a stronger VLM. Furthermore, by exploiting the inherent layout structure of documents, we partition each page into independent regions and apply our draft-verify strategy in parallel, assembling the final predictions according to the natural reading order. Extensive experiments demonstrate that our approach provides significant near-lossless speedups: it achieves a 2.42 $\times$  acceleration on v 1.5 for the dots.ocr model and up to 4.89 $\times$  acceleration on long-document parsing tasks. These results highlight the practicality and generality of our method, of-

fering a plug-and-play solution for accelerating VLM-based document parsers without architectural changes or retraining. We will release our code to facilitate reproducibility and encourage future research.

**Limitations and Future Work.** While our method achieves significant speedups, further engineering optimizations remain possible. We currently use FlexAttention [33] for customized attention masks in tree-structured verification, which is substantially faster than native attention but slower than highly optimized kernels like FlashAttention [10, 11]. Additional opportunities exist in efficient prefix tree construction and verification, as well as global GPU memory management [17], which could yield further acceleration beyond our current results. Additionally, our work focuses on document-parsing-specific designs that exploit layout structure and pipeline models. We have not comprehensively compared against general speculative decoding methods (e.g., Medusa [3], EAGLE [20, 21]) adapted to document parsing. While our domain-specific approach demonstrates strong performance, systematic comparison with general methods would provide valuable insights and is an important direction for future work. Nonetheless, our work demonstrates the substantial potential of speculative decoding for document intelligence, where natural layout structure and structured outputs create particularly favorable conditions for acceleration.

## References

- [1] Jean-Baptiste Alayrac, Jeff Donahue, Pauline Luc, Antoine Miech, Iain Barr, Yana Hasson, Karel Lenc, Arthur Mensch, Katherine Millican, Malcolm Reynolds, et al. Flamingo: a visual language model for few-shot learning. *NeurIPS*, 2022. 1
- [2] Lukas Blecher, Guillem Cucurull, Thomas Scialom, and Robert Stojnic. Nougar: Neural optical understanding for academic documents. *arXiv preprint arXiv:2308.13418*, 2023. 1, 3
- [3] Tianle Cai, Yuhong Li, Zhengyang Geng, Hongwu Peng, Jason D. Lee, Deming Chen, and Tri Dao. Medusa: Simple LLM inference acceleration framework with multiple decoding heads. In *ICML*, pages 5209–5235. PMLR, 2024. 3, 10
- [4] chatdoc com. Ocrflux. <https://github.com/chatdoc-com/OCRFlux>, 2025. Accessed:2025-11-10. 3
- [5] Charlie Chen, Sebastian Borgeaud, Geoffrey Irving, Jean-Baptiste Lespiau, Laurent Sifre, and John Jumper. Accelerating Large Language Model Decoding with Speculative Sampling. *arXiv preprint arXiv:2302.01318*, 2023. 2, 3, 8
- [6] Song Chen, Xinyu Guo, Yadong Li, Tao Zhang, Mingan Lin, Dongdong Kuang, Youwei Zhang, Lingfeng Ming, Fengyu Zhang, Yuran Wang, et al. Ocean-OCR: Towards general OCR application via a vision-language model. *arXiv preprint arXiv:2501.15558*, 2025. 2, 3, 6
- [7] Xi Chen, Xiao Wang, Soravit Changpinyo, AJ Piergiovanni, Piotr Padlewski, Daniel Salz, Sebastian Goodman, Adam Grycner, Basil Mustafa, Lucas Beyer, et al. PaLI: A jointly-scaled multilingual language-image model. In *ICLR*, 2022. 1
- [8] Cheng Cui, Ting Sun, Suyin Liang, Tingquan Gao, Zelun Zhang, Jiaxuan Liu, Xueqing Wang, Changda Zhou, Hongen Liu, Manhui Lin, Yue Zhang, Yubo Zhang, Handong Zheng, Jing Zhang, Jun Zhang, Yi Liu, Dianhai Yu, and Yanjun Ma. PaddleOCR-VL: Boosting multilingual document parsing via a 0.9b ultra-compact vision-language model. *arXiv preprint arXiv:2510.14528*, 2025. 3
- [9] Cheng Cui, Ting Sun, Manhui Lin, Tingquan Gao, Yubo Zhang, Jiaxuan Liu, Xueqing Wang, Zelun Zhang, Changda Zhou, Hongen Liu, et al. PaddleOCR 3.0 Technical Report. *arXiv preprint arXiv:2507.05595*, 2025. 2, 7
- [10] Tri Dao. FlashAttention-2: Faster attention with better parallelism and work partitioning. In *ICLR*, 2024. 10
- [11] Tri Dao, Daniel Y. Fu, Stefano Ermon, Atri Rudra, and Christopher Ré. FlashAttention: Fast and memory-efficient exact attention with IO-awareness. In *NeurIPS*, 2022. 10
- [12] Mostafa Elhoushi, Akshat Shrivastava, Diana Liskovich, Basil Hosmer, Bram Wasti, Liangzhen Lai, Anas Mahmoud, Bilge Acun, Saurabh Agarwal, Ahmed Roman, Ahmed Aly, Beidi Chen, and Carole-Jean Wu. LayerSkip: Enabling early exit inference and self-speculative decoding. In *ACL*, pages 12622–12642, Bangkok, Thailand, 2024. Association for Computational Linguistics. 3
- [13] Hao Feng, Shu Wei, Xiang Fei, Wei Shi, Yingdong Han, Lei Liao, Jinghui Lu, Binghong Wu, Qi Liu, Chunhui Lin, et al. Dolphin: Document image parsing via heterogeneous anchor prompting. *arXiv preprint arXiv:2505.14059*, 2025. 1, 3
- [14] Mukul Gagrani, Raghav Goel, Wonseok Jeon, Junyoung Park, Mingu Lee, and Christopher Lott. On speculative decoding for multimodal large language models. In *CVPR Workshops*, pages 8285–8289, 2024. 3
- [15] Ari Holtzman, Jan Buys, Li Du, Maxwell Forbes, and Yejin Choi. The curious case of neural text degeneration. In *ICLR*, 2020. 8, 13
- [16] Jialiang Kang, Han Shu, Wenshuo Li, Yingjie Zhai, and Xinghao Chen. ViSpec: Accelerating vision-language models with vision-aware speculative decoding. In *NeurIPS*, 2025. 3, 8
- [17] Woosuk Kwon, Zhuohan Li, Siyuan Zhuang, Ying Sheng, Lianmin Zheng, Cody Hao Yu, Joseph E. Gonzalez, Hao Zhang, and Ion Stoica. Efficient memory management for large language model serving with PagedAttention. In *SOSP*, 2023. 10
- [18] Yaniv Leviathan, Matan Kalman, and Yossi Matias. Fast inference from transformers via speculative decoding. In *ICML*, pages 19274–19286. PMLR, 2023. 2, 3
- [19] Junnan Li, Dongxu Li, Caiming Xiong, and Steven Hoi. BLIP: Bootstrapping language-image pre-training for unified vision-language understanding and generation. In *ICML*, 2022. 1
- [20] Yuhui Li, Fangyun Wei, Chao Zhang, and Hongyang Zhang. EAGLE: Speculative sampling requires rethinking feature uncertainty. In *ICML*, pages 28935–28948. PMLR, 2024. 3, 10

[21] Yuhui Li, Fangyun Wei, Chao Zhang, and Hongyang Zhang. EAGLE-2: Faster inference of language models with dynamic draft trees. In *EMNLP*, pages 7421–7432, Miami, Florida, USA, 2024. Association for Computational Linguistics. 3, 10

[22] Zhang Li, Yuliang Liu, Qiang Liu, Zhiyin Ma, Ziyang Zhang, Shuo Zhang, Zidun Guo, Jiarui Zhang, Xinyu Wang, and Xiang Bai. MonkeyOCR: Document parsing with a structure-recognition-relation triplet paradigm. *arXiv preprint arXiv:2506.05218*, 2025. 1, 3

[23] Luxi Lin, Zhihang Lin, Zhanpeng Zeng, and Rongrong Ji. Speculative decoding reimaged for multimodal large language models. *arXiv preprint arXiv:2505.14260*, 2025. 3

[24] Haotian Liu, Chunyuan Li, Yuheng Li, and Yong Jae Lee. Improved baselines with visual instruction tuning. *arXiv:2310.03744*, 2023. 1

[25] Yuan Liu, Zhongyin Zhao, Le Tian, Haicheng Wang, Xubing Ye, Yangxiu You, Zilin Yu, Chuhan Wu, Xiao Zhou, Yang Yu, et al. POINTS-Reader: Distillation-free adaptation of vision-language models for document conversion. *arXiv preprint arXiv:2509.01215*, 2025. 3

[26] Nikolaos Livathinos, Christoph Auer, Maksym Lysak, Ahmed Nassar, Michele Dolfi, Panos Vagenas, Caesar Berrospi Ramis, Matteo Omenetti, Kasper Dinkla, Yusik Kim, et al. Docling: An efficient open-source toolkit for AI-driven document conversion. *arXiv preprint arXiv:2501.17887*, 2025. 1, 2

[27] Souvik Mandalm. Nanonets-ocr-s. <https://nanonets.com/research/nanonets-ocr-s/>, 2025. Accessed:2025-11-10. 2

[28] Xupeng Miao, Gabriele Oliaro, Zhihao Zhang, Xinhao Cheng, Zeyu Wang, Zhengxin Zhang, Rae Ying Yee Wong, Alan Zhu, Lijie Yang, Xiaoxiang Shi, Chunhan Shi, Zhuoming Chen, Daiyaan Arfeen, Reyna Abhyankar, and Zhihao Jia. SpecInfer: Accelerating large language model serving with tree-based speculative inference and verification. In *AS-PLOS*, page 932–949, 2024. 3

[29] Junbo Niu, Zheng Liu, Zhuangcheng Gu, Bin Wang, Linke Ouyang, Zhiyuan Zhao, Tao Chu, Tianyao He, Fan Wu, Qintong Zhang, Zhenjiang Jin, Guang Liang, Rui Zhang, Wenzheng Zhang, Yuan Qu, Zhifei Ren, Yuefeng Sun, Yuanhong Zheng, Dongsheng Ma, Zirui Tang, Boyu Niu, Ziyang Miao, Hejun Dong, Siyi Qian, Junyuan Zhang, Jingzhou Chen, Fangdong Wang, Xiaomeng Zhao, Liqun Wei, Wei Li, Shasha Wang, Ruiliang Xu, Yuanyuan Cao, Lu Chen, Qianqian Wu, Huaiyu Gu, Lindong Lu, Keming Wang, Dechen Lin, Guanlin Shen, Xuanhe Zhou, Linfeng Zhang, Yuhang Zang, Xiaoyi Dong, Jiaqi Wang, Bo Zhang, Lei Bai, Pei Chu, Weijia Li, Jiang Wu, Lijun Wu, Zhenxiang Li, Guangyu Wang, Zhongying Tu, Chao Xu, Kai Chen, Yu Qiao, Bowen Zhou, Dahua Lin, Wentao Zhang, and Conghui He. MinerU2.5: A decoupled vision-language model for efficient high-resolution document parsing. *arXiv preprint arXiv:2509.22186*, 2025. 1, 2, 3, 6

[30] Vik Paruchuri. Marker. <https://github.com/datalab-to/marker>, 2025. Accessed:2025-11-10. 1, 2

[31] Jake Poznanski, Aman Rangapur, Jon Borchardt, Jason Dunkelberger, Regan Huff, Daniel Lin, Christopher Wilhelms, Kyle Lo, and Luca Soldaini. olmOCR: Unlocking trillions of tokens in PDFs with vision language models. *arXiv preprint arXiv:2502.18443*, 2025. 1, 2, 3, 6

[32] Jake Poznanski, Luca Soldaini, and Kyle Lo. olmOCR 2: Unit test rewards for document OCR. *arXiv preprint arXiv:2510.19817*, 2025. 2, 3

[33] Team PyTorch. FlexAttention: The flexibility of pytorch with the performance of flashattention. <https://pytorch.org/blog/flexattention/>, 2025. Accessed:2025-11-10. 7, 10

[34] rednote. dots.ocr: Multilingual document layout parsing in a single vision-language model. <https://github.com/rednote-hilab/dots.ocr>, 2025. Accessed:2025-11-10. 2, 3, 6

[35] Xin Sun, Tao Ge, Furu Wei, and Houfeng Wang. Instantaneous grammatical error correction with shallow aggressive decoding. *arXiv preprint arXiv:2106.04970*, 2021. 3

[36] Ruslan Svirchevski, Avner May, Zhuoming Chen, Beidi Chen, Zhihao Jia, and Max Ryabinin. SpecExec: Massively parallel speculative decoding for interactive LLM inference on consumer devices. *arXiv preprint arXiv:2406.02532*, 2024. 2

[37] Hunyuan Vision Team, Pengyuan Lyu, Xingyu Wan, Gengluo Li, Shangpin Peng, Weinong Wang, Liang Wu, Huawei Shen, Yu Zhou, Canhui Tang, Qi Yang, Qiming Peng, Bin Luo, Hower Yang, Xinsong Zhang, Jinnian Zhang, Houwen Peng, Hongming Yang, Senhao Xie, Longsha Zhou, Ge Pei, Binghong Wu, Rui Yan, Kan Wu, Jieneng Yang, Bochao Wang, Kai Liu, Jianchen Zhu, Jie Jiang, Linus, Han Hu, and Chengquan Zhang. HunyuanOCR Technical Report. *arXiv preprint arXiv:2511.19575*, 2025. 2, 3, 6

[38] Mistral AI Team. Mistral-ocr. [https://mistral.ai/news/mistral-ocr?utm\\_source=ai-bot.cn](https://mistral.ai/news/mistral-ocr?utm_source=ai-bot.cn), 2025. Accessed:2025-11-10. 1

[39] Qwen Team. Qwen3-VL. <https://github.com/QwenLM/Qwen3-VL>, 2025. Accessed:2025-11-10. 2, 6

[40] Bin Wang, Chao Xu, Xiaomeng Zhao, Linke Ouyang, Fan Wu, Zhiyuan Zhao, Rui Xu, Kaiwen Liu, Yuan Qu, Fukai Shang, et al. MinerU: An open-source solution for precise document content extraction. *arXiv preprint arXiv:2409.18839*, 2024. 1, 2, 7

[41] Baode Wang, Biao Wu, Weizhen Li, Meng Fang, Zuming Huang, Jun Huang, Haozhe Wang, Yanjie Liang, Ling Chen, Wei Chu, and Yuan Qi. Infinity Parser: Layout aware reinforcement learning for scanned document parsing. *arXiv preprint arXiv:2506.03197*, 2025. 2, 3

[42] Haoran Wei, Chenglong Liu, Jinyue Chen, Jia Wang, Lingyu Kong, Yanming Xu, Zheng Ge, Liang Zhao, Jianjian Sun, Yuang Peng, et al. General OCR Theory: Towards OCR-2.0 via a unified end-to-end model. *arXiv preprint arXiv:2409.01704*, 2024. 1, 3

[43] Haoran Wei, Yaofeng Sun, and Yukun Li. DeepSeek-OCR: Contexts optical compression. *arXiv preprint arXiv:2510.18234*, 2025. 3, 9

[44] Thomas Wolf, Lysandre Debut, Victor Sanh, Julien Chauvin, Clement Delangue, Anthony Moi, Pierrick Cistac, Tim Rault, Remi Louf, Morgan Funtowicz, Joe Davison, Sam

Shleifer, Patrick von Platen, Clara Ma, Yacine Jernite, Julien Plu, Canwen Xu, Teven Le Scao, Sylvain Gugger, Mariama Drame, Quentin Lhoest, and Alexander Rush. Transformers: State-of-the-art natural language processing. In *ACL*, pages 38–45, 2020. [6](#)

[45] Zhinan Xie, Peisong Wang, and Jian Cheng. HiViS: Hiding visual tokens from the drafter for speculative decoding in vision-language models. *arXiv preprint arXiv:2509.23928*, 2025. [3](#)

[46] Jin Xu, Xiaojiang Liu, Jianhao Yan, Deng Cai, Huayang Li, and Jian Li. Learning to break the loop: Analyzing and mitigating repetitions for neural text generation. In *NeurIPS*, pages 3082–3095, 2022. [13](#)

[47] Jun Zhang, Jue Wang, Huan Li, Lidan Shou, Ke Chen, Gang Chen, and Sharad Mehrotra. Draft & Verify: Lossless large language model acceleration via self-speculative decoding. *arXiv preprint arXiv:2309.08168*, 2023. [2](#)

[48] Qintong Zhang, Bin Wang, Victor Shea-Jay Huang, Junyuan Zhang, Zhengren Wang, Hao Liang, Conghui He, and Wentao Zhang. Document parsing unveiled: Techniques, challenges, and prospects for structured information extraction. *arXiv preprint arXiv:2410.21169*, 2024. [1](#)

[49] Weilin Zhao, Yuxiang Huang, Xu Han, Chaojun Xiao, Zhiyuan Liu, and Maosong Sun. Ouroboros: Speculative decoding with large model enhanced drafting. *arXiv preprint arXiv:2402.13720*, 2024. [3](#)

# Training-Free Acceleration for Document Parsing Vision-Language Model with Hierarchical Speculative Decoding

## Supplementary Material

### A. Length Bias in Qwen3-VL Evaluation

Document parsing requires the model to faithfully reconstruct textual content, formulas, tables, and other structural elements. These structures—especially mathematical expressions and tables—tend to contain highly repetitive patterns. Such repetition can cause models to over-emphasize formatting cues while neglecting semantic content, ultimately leading to *repetition hallucination* as shown in Fig. A1, which has been emphasized in the previous studies [15, 46]. This issue tends to be more pronounced in general-purpose models that are not specifically tailored for document parsing, such as Qwen3-VL. Once a model falls into this mode of degeneration, its generated output becomes unreliable and no longer reflects the actual effectiveness of our method. For this reason, we restricted Qwen3-VL to a maximum generation length of 2048 tokens and excluded samples exhibiting severe repetition hallucination when reporting speed measurements in Tab. 1 and Tab. 2 of the main paper.

However, while the 2048-token limit prevents obvious long-sequence degradation, it also confines the evaluation to a “short-generation regime,” which may obscure the acceleration behavior that emerges in realistic long-document parsing scenarios. To be more rigorous, we extended the maximum generation length to 8192 tokens and again filtered out samples affected by repetition hallucination, and then evaluated the end-to-end acceleration of Qwen3-VL under this more comprehensive setting.

The results on OmniDocBench v1.5 and olmOCR-Bench are summarized in Tabs. A1 and A2 respectively. Overall, our method achieves acceleration comparable to that reported in the main paper, and the improvement becomes even more apparent in extremely long and dense text scenarios such as the Newspaper category. This further demonstrates the advantage of our pipeline in handling high-volume, tightly packed document content. On the other hand, when extending the generation length, the longer context may introduce unpredictable stylistic deviations between the model’s output and the draft. In such cases, the draft may not be accepted, leading to fluctuations in the measured speedup.

### B. Qualitative Analysis

We qualitatively analyze the factors that dominate the acceleration behavior of our hierarchical speculative decoding (HSD). Specifically, we compare representative pages

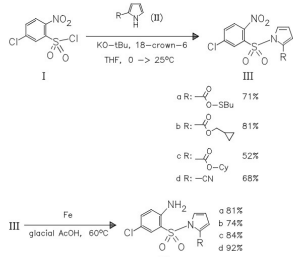
with *high* end-to-end speedups against those with *limited* speedups. Across datasets, we observe two recurring bottlenecks for low-speedup cases: (i) **draft-limited** pages where region/page drafts are inaccurate and thus frequently rejected, and (ii) **prefill-dominated** pages where the fixed vision/prefill cost accounts for a large portion of the total latency, making decode-side acceleration less visible in end-to-end measurements. Here, *vision/prefill* denotes the front-end stage including the image encoder forward pass and the subsequent multimodal prefill for KV-cache construction.

**High-speedup cases: accurate drafts and decode-dominated latency.** Figs. A2 and A3 shows typical pages with large speedups (e.g., financial reports, newspapers, or well-structured multi-column layouts). These pages share two properties. First, the pipeline produces high-quality region and page drafts that match the target model’s output up to minor formatting variations. As a result, the verifier accepts long consecutive draft segments, yielding a high AAL and few rollbacks. Second, these pages usually contain substantial textual content, so the decode loop constitutes a major part of the overall latency. The fixed vision/prefill cost is amortized over many decoding steps, allowing the decode-side gains to translate directly into strong end-to-end acceleration (high  $SR_{e2e}$ ). This evidences that HSD approaches its theoretical benefit when drafts are reliable and decoding dominates the runtime.

**Low-speedup cases I: draft-limited pages.** In contrast, Fig. A4 shows a representative low-speedup case where acceleration is limited by draft quality. The pipeline draft contains many token-level errors, including missing words and noisy character predictions, which commonly arise when the pipeline struggles with cursive handwriting. These errors induce frequent mismatches during verification, resulting in short accepted spans and repeated rollbacks. Consequently, AAL remains low and the target model must perform substantial autoregressive corrections, limiting  $SR_{e2e}$ . This case highlights that draft accuracy is a primary upper bound on speculative speedup: when drafts are heavily corrupted, the verifier cannot reliably accept long segments and thus cannot effectively skip decoding steps.

**Low-speedup cases II: prefill-dominated pages.** A second failure mode arises from pages where the end-to-end latency is bottlenecked by the fixed vision/prefill stage once decoding is accelerated. As shown in Fig. A5, such pages

Anti-HIV-1 Activity of Pyrrol Aryl Sulfone (PAS) Derivatives: Synthesis and SAR Studies of Novel Esters and Amides at the Position 2 of the Pyrrole Nucleus. — Of all tested compounds, compound (IVa) shows the highest antiviral activity. — (SILVESTRI\*, R.; ARTICO, M.; LA REGINA, G.; DE MARTINO, G.; LA COLLA, M.; LODDO, R.; COLLA\*, P.; Farmaco 59 (2004) 3, 201-210; Dip. Stud. Farm., Univ. La Sapienza, I-00185 Roma, Italy; Eng.) — C. Oppel



(a) Input Page

(b) Prediction

Figure A1. Illustration of the repetition hallucination.

Table A1. Acceleration of Qwen3-VL on OmniDocBench v1.5 when filtering out samples  $> 8192$  tokens. Results are reported for our proposed hierarchical speculative decoding. AAL denotes the average number of accepted draft tokens per verification step;  $SR_{decode}$  is the decode-only speedup (draft generation + verification);  $SR_{e2e}$  is the end-to-end page-level latency speedup (including vision/prefill stages).

Model	Parameters	Overall			$SR_{e2e}$	Academic Papers	Book	Textbook	Exam Papers	Magazine	Newspaper	Notes	Financial Report
		AAL	$SR_{decode}$	$SR_{e2e}$									
Qwen3-VL-8B	9B	4.98 $\times$	2.61 $\times$	2.62 $\times$	1.63 $\times$	2.56 $\times$	2.29 $\times$	2.02 $\times$	2.18 $\times$	2.59 $\times$	4.62 $\times$	1.86 $\times$	1.91 $\times$
Qwen3-VL-2B	2B	4.33 $\times$	2.18 $\times$	2.18 $\times$	1.35 $\times$	2.13 $\times$	1.82 $\times$	1.87 $\times$	2.04 $\times$	2.61 $\times$	4.03 $\times$	1.69 $\times$	1.75 $\times$

Table A2. Acceleration of Qwen3-VL on olmOCR-Bench when filtering out samples  $> 8192$  tokens.

Model	Parameters	Overall			$SR_{e2e}$	arXiv Math	Old Scans Math	Tables	Old Scans	Headers Footers	Multi Column	Long Tiny Text
		AAL	$SR_{decode}$	$SR_{e2e}$								
Qwen3-VL-8B	9B	4.08 $\times$	2.40 $\times$	2.42 $\times$	2.51 $\times$	1.64 $\times$	1.60 $\times$	1.11 $\times$	2.65 $\times$	3.75 $\times$	2.19 $\times$	
Qwen3-VL-2B	2B	4.89 $\times$	2.97 $\times$	2.98 $\times$	3.00 $\times$	1.65 $\times$	2.20 $\times$	1.46 $\times$	3.20 $\times$	4.48 $\times$	2.54 $\times$	

typically have short or sparse outputs, leaving limited decoding time to amortize the front-end cost. Even when HSD greatly reduces the decode loop, the overall runtime remains constrained by vision/prefill, so the end-to-end improvement is capped. This explains the smaller gains observed for short documents in our quantitative results: decode-side acceleration alone cannot overcome a front-end cost that occupies a significant fraction of the inference budget.

**Takeaways.** The qualitative evidence supports two key conclusions. First, draft quality governs AAL and decode-side acceleration: accurate drafts enable long accepted spans and large reductions in decoding steps, whereas draft errors cause frequent rejections and limited gains. Second, the latency composition governs end-to-end speedup: when the fixed vision/prefill stage accounts for a substantial fraction of total runtime (as in short or sparse pages), decode-side improvements translate only partially to  $SR_{e2e}$ .

Taken together, these findings explain why HSD delivers robust overall acceleration while exhibiting predictable, interpretable variation across document types.



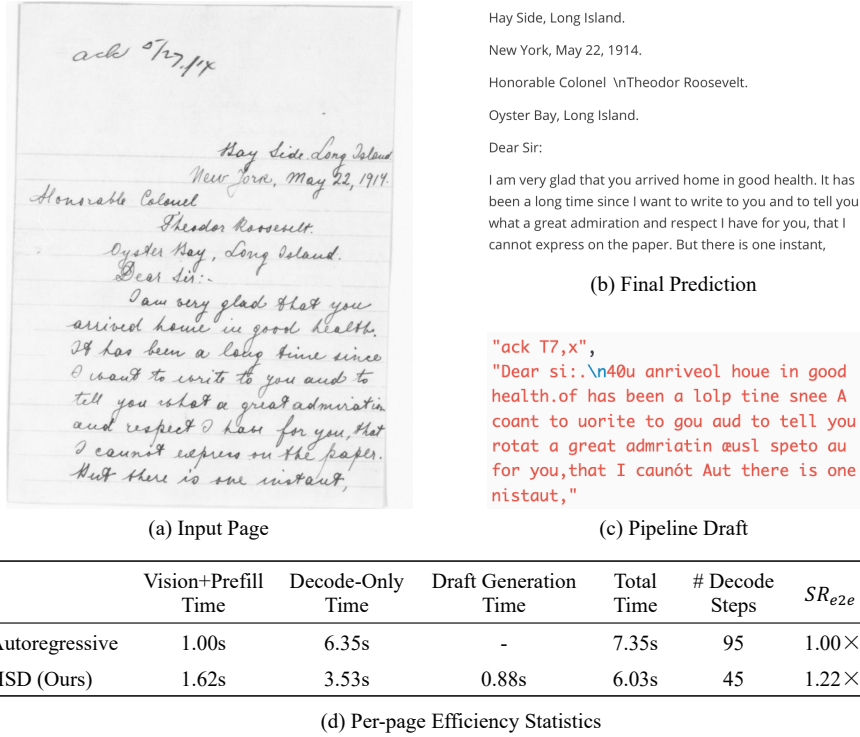


Figure A4. Draft-limited low-speedup example. Draft errors lead to frequent rejections and low AAL.

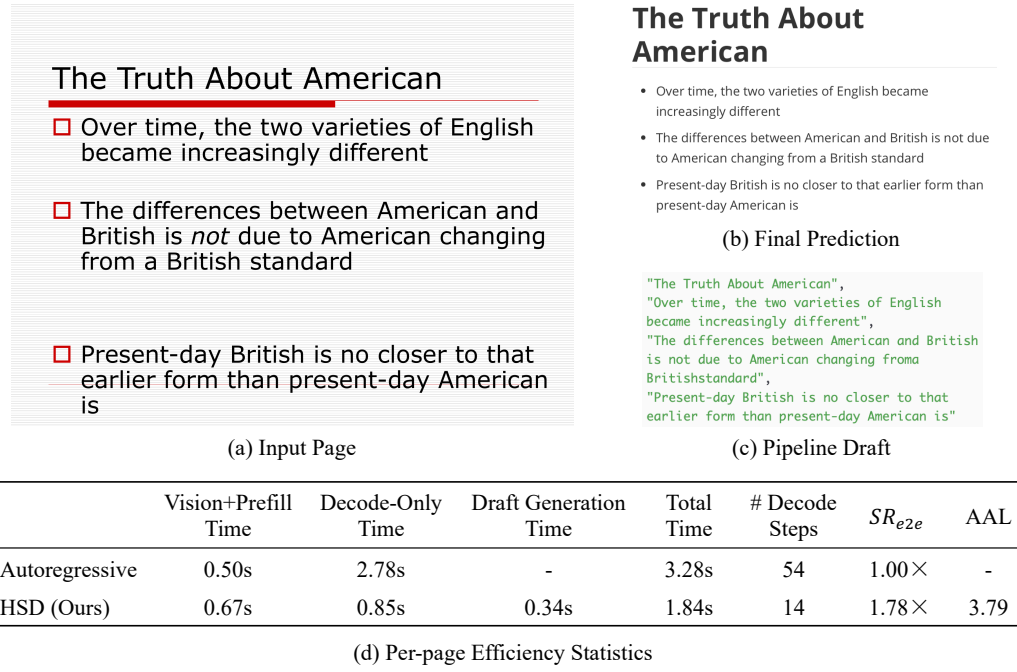


Figure A5. Prefill-dominated low-speedup example. Despite decode-side gains, large fixed vision/prefill cost limits  $SR_{e2e}$ .